

A DC/AC CONVERTER FOR SINGLE-PHASE GRID-CONNECTED PHOTOVOLTAIC SYSTEMS

Souza, Kleber and Antunes, Fernando
Energy Processing and Control Group - GPEC
Universidade Federal do Ceará
ksouza@dee.ufc.br; fantunes@dee.ufc.br

Abstract – This work proposes a static DC/AC converter for grid-connected PV systems. The DC/AC converter system is made of a current fed Push-Pull converter and an inverter. Both converters operate with constant switching frequency. The design, principle of operation, control circuits and the characteristics of the system are presented. In addition to the theoretical analysis, simulation results are shown to validate the principle of operation of the converter as part of a grid-connected system.

I. INTRODUCTION

The solar energy is today a clean and viable source of electricity. It has been used as the main source for electrical loads in rural areas away from the grid or grid-connected in distributed energy production. Used only in satellite and space applications in the past, photovoltaic systems have come down to Earth, and its use is spreading all over the world. Although the cost of such systems is still regarded as high, the continuous research in power electronics and in the physics of semiconductors has pointed towards cost reduction of PV systems.

The large use of PV systems to produce electric energy since 1990 in countries like Germany, Denmark, Japan and USA has made the photovoltaic energy to be part of the national grid. Grid-connected PV systems have increased with an annual rate over 25%. This is related to the ever increasing use of small grid-connected systems as part of reduction of load demand from the grid. Within the PV market the one for grid-connected applications is the fastest spread one.

Grid-connected PV systems can be of two types: centralized generation or integrated to urban building. In the first case, the photovoltaic plant is located away of urban centers due to the necessity of relatively large areas. In the second case the systems are integrated to urban buildings commonly located on roofs.

Grid-connected PV systems neither require batteries or to be oversized to attend peak demands because the grid is a large storage energy system. If the PV system generates energy in excess to the residential load, the excess is sold to the grid. When the PV system generates less energy than the value required by the load, the grid supplies the extra value. Grid-connected PV system, due to its modularity, short period between the installation of the plant and the beginning of operation, could be very attractive for the utility [3].

In urban areas the intense use of air conditioning to climatise rooms has a straight relation with high solar irradiation. This means more photovoltaic energy generation. In that case, grid connected PV systems are na advantage for the local utility which can alleviate high peaks of demand, thus increasing the capacity of the transmission systems and distribution and postponing the

great investments and long periods of installation of new lines.

Several papers have been published related to the application of static converters in PV systems. In [6] it is presented a 5kW grid connected system which power processing unit is composed by a DC-DC series resonant converter, a high frequency transformer and a full-bridge inverter. Even though, with a capacity of processing high power, this converter has the disadvantage of the use of a large number of power switches.

A conversion system made of two full-bridge inverters, without a transformer, for grid-connected PV system in introduced in [7]. The absence of the transformer is justified by a higher efficiency and lower weight and volume. However, the PV array is not isolated from the grid.

Many others papers have been published in the field of grid-connected PV systems [2, 3, 4 e 5]. They are very interesting however in which either the power stage or the isolation stage operates in low frequency. Other works found in the literature deal with PV systems with many power stages, which compromise the efficiency of the system. It is with the objective to reduce or even to solve such problems that in this work it is presented a simple, robust and naturally insulated structure. It is composed by current fed Push-Pull converter and an inverter. Both converters operate in high frequency.

II. THE PROPOSED DC/AC SYSTEM

Fig.01 illustrates the current-fed push-pull converter. It guarantees the galvanic isolation between the PV modules and the grid as well as provides the necessary voltage level at the input of the second stage.

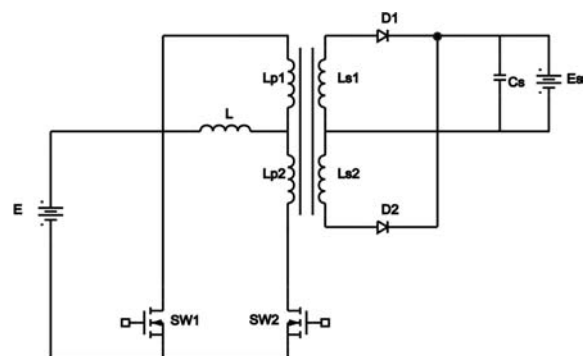


Fig. 1 – The DC/DC converter.

The second stage, a full bridge inverter, is shown in Fig.02. It generates a sinusoidal current, with low harmonic distortion and with 180° out of phase with the grid voltage.

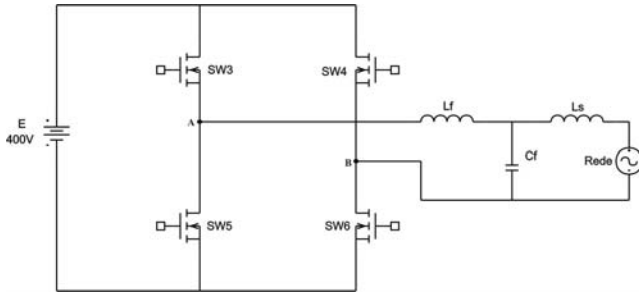


Fig. 2 – The inverter output stage.

III. STEADY-STATE ANALYSIS OF THE DC/DC CONVERTER

For the purpose of this analysis the converter is considered to be in steady-state condition, the switches are ideal and the transformer is also ideal.

The stages of operation are described as follows:

First stage (t_0, t_1): The following initial conditions are assumed: switch SW1 is on, the value of the inductor current is I_m and the output capacitor (C_s) is fully charged. At instant t_0 , SW2 is driven on and takes half on the value of the input inductor current. The transformer windings have such direction that for both SW1 and SW2 on the flux produced by each winding are opposite and consequently the net voltage across the windings is zero. Fig.03(a) shows the equivalent circuit for the first stage. During this stage the input inductor current rises linearly until SW1 is driven off. During stage one there is energy transfer to the load, which is supplied by the output capacitor. This stage ends when the input inductor current has a value I_m .

Second stage (t_1, t_2): At instant t_1 , SW1 is driven on. D1 starts to conduct enforcing to the input inductor the load voltage referred to the primary minus the input voltage. The load voltage referred to the primary side is essentially higher than the input voltage to guarantee the energy balance in the inductor. During this stage the energy is transferred to the load via input inductor which discharges linearly. At t_2 the input inductor current reaches the starting value of stage one: I_m . Fig.3(b) present the equivalent circuit for this stage.

Third stage (t_2, t_3): In the instant the switch SW1 is driven on and the converter assumes an identical configuration, including the inductor initial current, of the first stage. Fig.3(c) present the equivalent circuit for this stage.

Fourth stage (t_3, t_4): In the instant t_3 , the switch SW2 is driven off, and the diode D2 starts to conduct. The imposed voltage across the input voltage is identical to the second stage, however the polarity in the transformer windings is opposite. The transferred energy and the initial and final levels of current in the inductor are identical to the second stage. Fig.3(d) present the equivalent circuit for this stage.

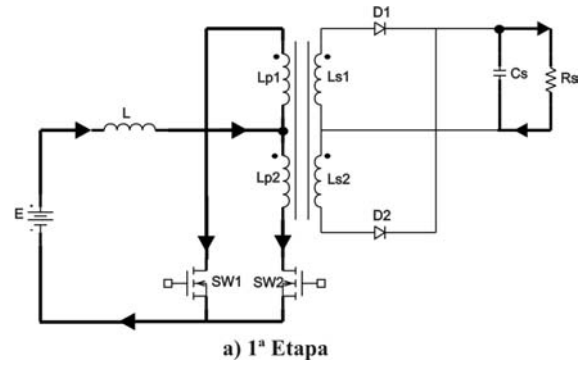


Fig. 3(a) – 1st stage of operation.

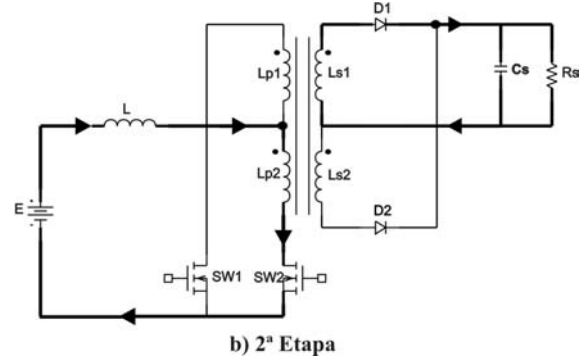


Fig. 4(b) – 2nd stage of operation.

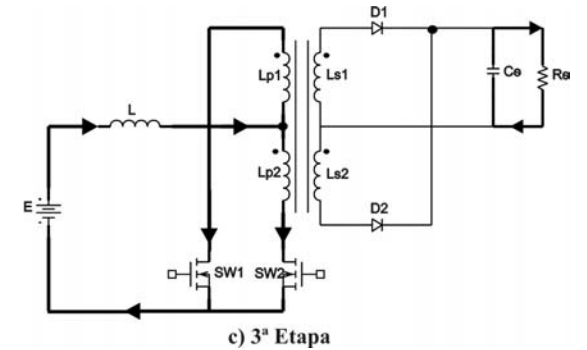


Fig. 5(c) – 3rd stage of operation.

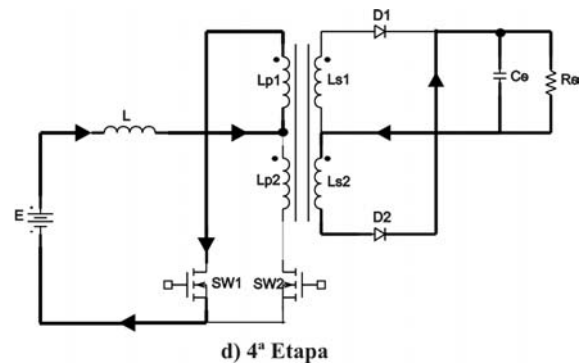


Fig. 6(d) – 4th stage of operation.

Fig. 7 shows the drive signals of the DC/DC converter. As illustrated, there are four operation stages. In the first and in the third stages, the converter works accumulating energy in the input inductor. In Fig.04 these stages happen when the switches are simultaneously on (the first stage occurs from t_0 to t_1 and the second occurs from t_2 to t_3). The

duration of time of these stages is the same and referred to as Δt_A . On the other hand in the second and fourth stages, the converter transfers energy to the secondary. In Fig.04 these stages occur when just one of the switches is on (the second stage occurs from t_1 to t_2 and the fourth occurs from t_3 to t_4). The duration of time of these stages is the same and referred to as Δt_d .

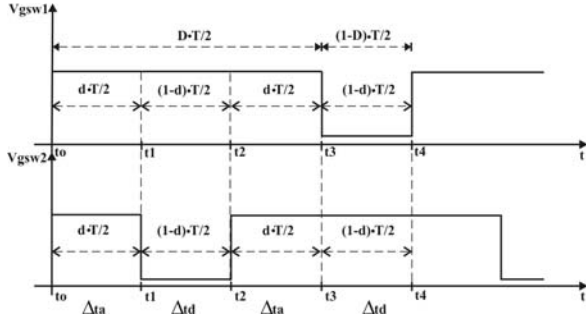


Fig. 7 - Drive signals of the DC/DC converter.

Due to the current-fed characteristic, the switches SW1 and SW2 can not keep up opened simultaneously. The Push-Pull converter operates in continuous condition mode with constant frequency, and its duty cycle is defined by (1), where T represents the switching period of the converter.

$$D = \frac{2 \cdot \Delta t_a}{T} \quad (1)$$

IV. PUSH-PULL DRIVE AND CONTROL CIRCUITS

As the current fed Push-Pull converter works with a duty cycle above 50% and with the drive signals 180° out of phase, a dedicated drive circuit has been developed for it was not possible to find one off the shelf, with the desired features. Fig.05 presents the circuit diagram of the implemented circuit.

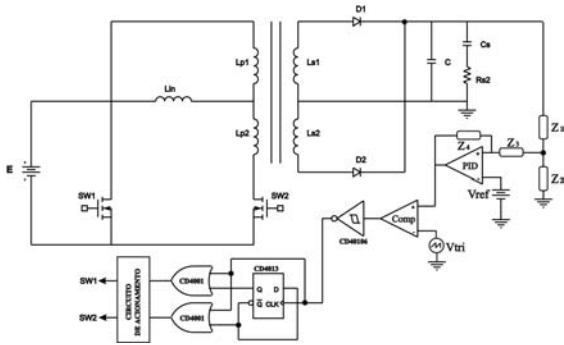


Fig. 8 – Drive and control circuit.

The closed loop control of the converter is realized by a PID controller. The implemented control loop makes constant the magnitude of the output voltage for load changes or changes on the input voltage. The controller as well as the comparator have been implemented with the UNITRODE™ IC 3524. That IC is dedicated for the generation PWM signals owing to an internal compensator, a comparator, sawtooth waveform circuit generator. The IC

has also protection against short circuit and two independent signal output with a duty cycle limited to 0.5. As the converter operates with a duty cycle higher than 50%, some external circuits have been added in order to make the two independent output signals in just one but with the possibility to operate with a duty cycle within 0 to 100%.

For the generation of the push-pull converter drive signals out of phase of 180° between them another logic circuit using D flip-flop and two logic gates OR has been implemented. Fig.6 illustrates the circuit.

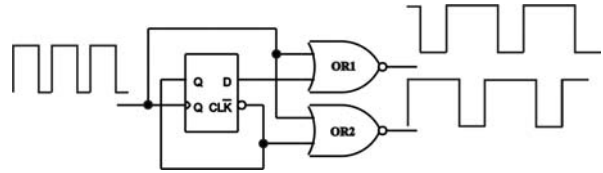


Fig. 9 – Circuit generator of the phase shift between the drive signals.

The implemented circuit is simple and its operation can be understood by Fig.7. The D flip-flop changes its output level at the rising transition of the clock. So, the flip-flop Q output has a signal with half of the period of the clock signal and with 50% duty cycle. Q and \bar{Q} are compared with the clock signal in two OR logic gates. This results in two signals identical to the clock signal but 180° out of phase between each other.

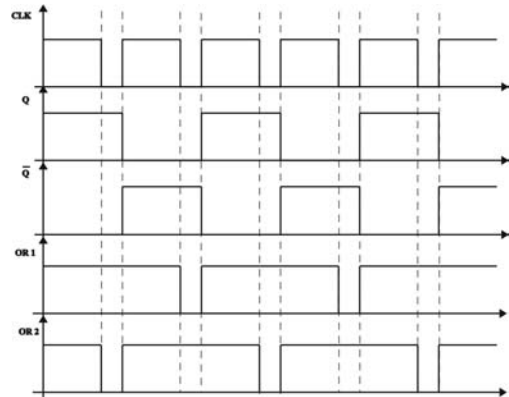


Fig. 10 – Phase-shift generator main waveforms.

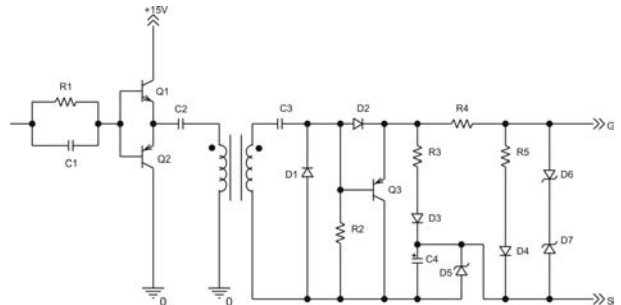


Fig. 11 – Drive signal circuit with the pulse transformer.

The drive circuit must allow an adequate operation of the switch during the stages of commutation, turn on and turn off. It should also provide isolation between the control circuit and the power circuit. A well designed circuit leads the switches to operate with minimum losses and minimum voltage and current stresses. Fig.08 shows the designed

drive circuit that can provide a duty cycle within the range 0 to 1.

IV. STEADY-STATE ANALYSIS OF THE INVERTER

The three level modulation to with commutation of both arms has been implemented due it easy of implementation and it makes possible the output filter size reduction. Fig.09 shows the modulation used. A characteristic of this modulation is the utilization of two triangular waves (carriers) 180o out of phase from each other. Switches SW3 and SW5 are controlled by comparing the sinusoidal reference V_C with the triangular carrier 2. In the same fashion switches SW4 and SW6 are controlled by comparing the sinusoidal reference V_C with the triangular carrier 1. It should be pointed out that SW3 is activated when the sinusoidal reference is greater than the triangular carrier. In the same way, SW4 is activated when the sinusoidal reference is smaller than the triangular carrier. Fig.09 also illustrates that the output filter input voltage has a frequency of twice the value of the commutation frequency. This is a big advantage for the filter design. To follow it is presented the converter operation stages using this modulation..

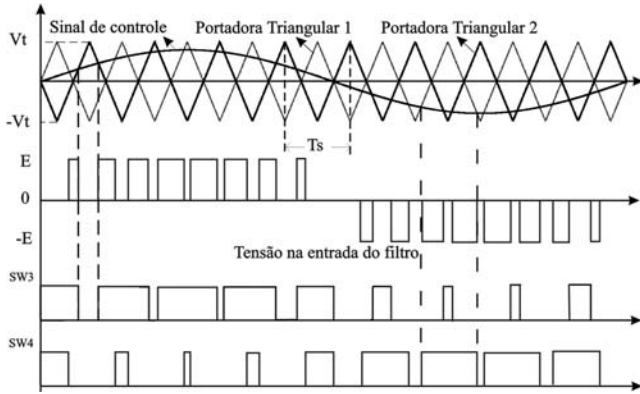


Fig. 12 – Three-level PWM modulation.

The passive components of the filter are determined by (2) and (3)

$$L_f = \frac{E_I \cdot \frac{E_I}{2 \cdot V_{C_{PK}}} - V_{C_{PK}} \cdot \left(\frac{E_I}{2 \cdot V_{C_{PK}}} \right)^2}{\Delta I_{max} \cdot 2 \cdot f_c} \cdot \frac{V_{C_{PK}}}{E_I} \quad (2)$$

Where E_I corresponds to the inverter input voltage, $V_{C_{PK}}$ the peak value of the filter capacitor voltage and f_c the frequency of commutation of the switches.

$$C_f = \frac{\left(\frac{10}{4 \cdot \pi \cdot f_c} \right)^2}{L_f} \quad (3)$$

Fig.10 shows the control and drive circuits.

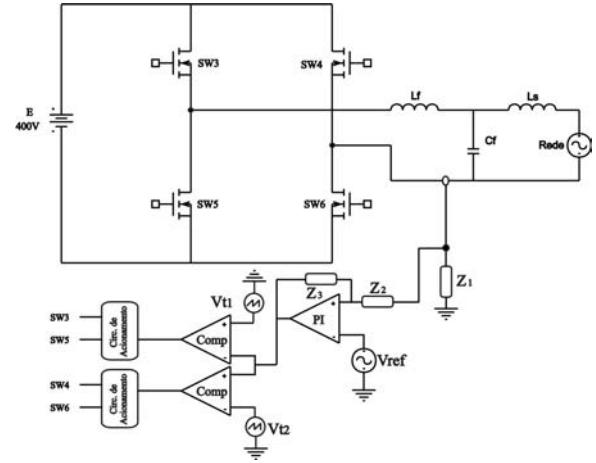


Fig. 13 – Drive circuit and control diagram of the inverter.

For the control loop, it has been used a PI controller. The aim of this control loop is to make the filter current to follow a reference sinusoidal signal and in phase with the grid voltage. This makes the inverter output current sinusoidal and with a controlled magnitude. The reference signal is generated by the microcontroller-implemented MPPT circuit. The circuit gets voltage and current samples from the panels, and based on the ration of the derivative of the voltage and the current, the circuit adjust the reference signal amplitude. The used algorithm was developed by Hussein in [8].

VII. EXPERIMENTAL RESULTS

The results presented here were obtained for the following design specification.

$E = 50V$	Voltage supplied by the solar panels
$E_s = 400V$	Voltage in the secondary transformer side
$P_{out} = 120W$	Output power
$f_o = 60Hz$	Output current frequency
$f_s = 40kHz$	Switching frequency

The Fig. 14 shows the waveform current in the input inductor of the Push-Pull converter.

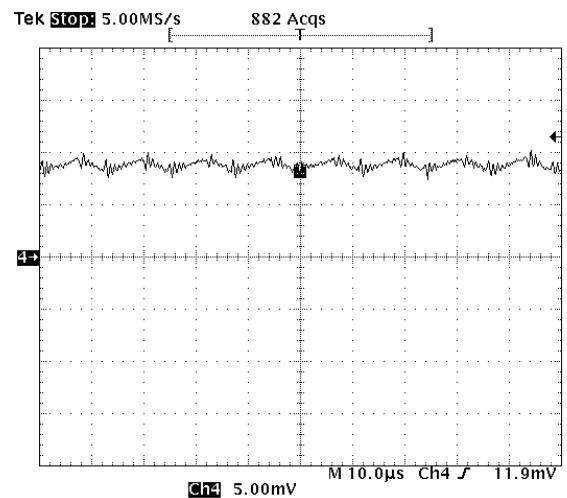


Fig. 14 – Push-Pull inductor current
Scale: 2.5 A/Div; 10 µs/Div.

Fig.12 shows the control signal voltage across the gate-source of one MOSFET of the push-pull converter.

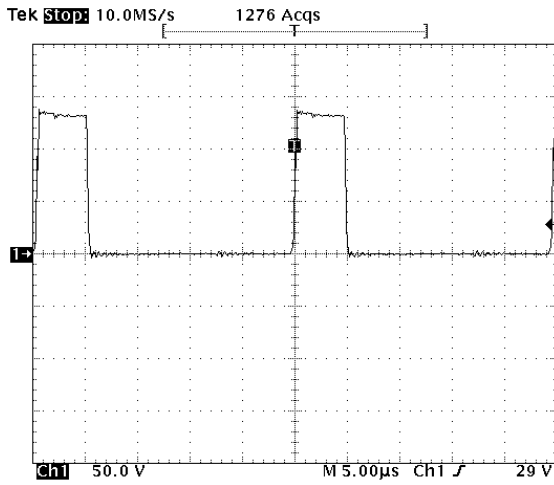


Fig. 15 – Drain-Source voltage of SW2.
Scale: 50 V/Div; 5 μ s/Div.

Fig. 16 shows the current waveform of one MOSFET of the push-pull converter.

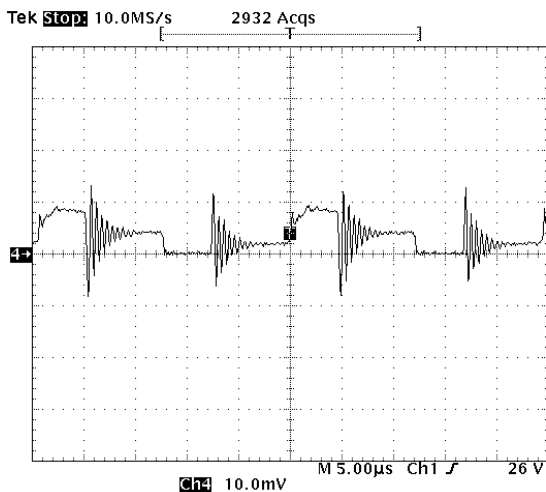


Fig. 16 - current waveform of SW2.
Scale: 5 A/Div; 5 μ s/Div.

The damped high frequency signals in the switch current shown in Fig.13 are caused by the transformer leakage inductance and stray capacitances, and, to certain extension by the secondary diodes reverse recovery time.

Fig.14 shows the waveform of the inverter output current and the grid voltage waveform.

As can be seen the PV systems generated current is 180° out of phase from the grid voltage. This shows that the PV system is feeding the grid.

Fig.15 and Fig.16 show the harmonic spectra of the grid voltage and the injected current.

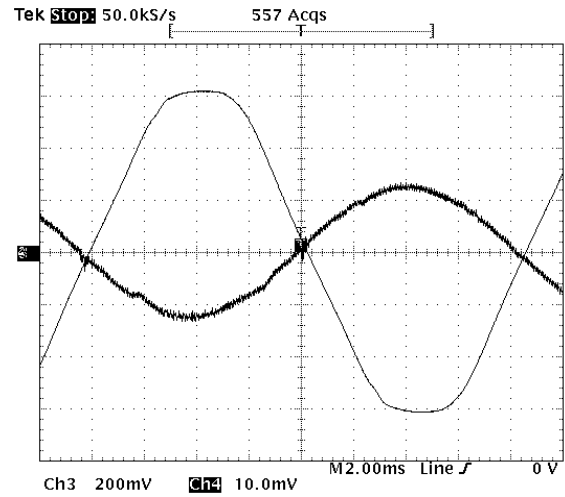


Fig. 17 - Inverter output current and the grid voltage waveforms.
Scales: 100 V/Div; 500 mA/Div; 2 ms/Div.

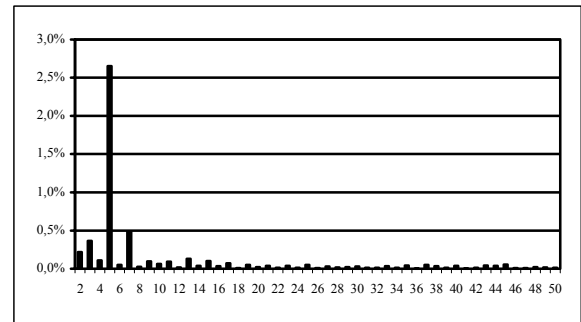


Fig. 18 harmonic spectrum of the grid voltage with a THD = 2,73%.

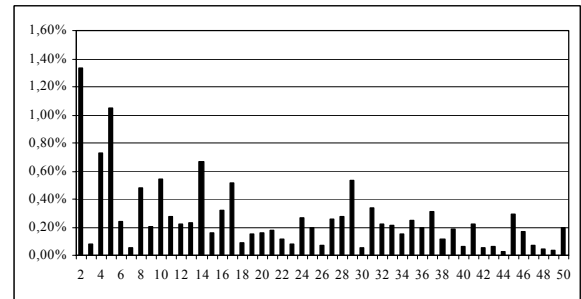


Fig. 19 harmonic spectrum of the injected current. TDH = 1,81%.

VIII. CONCLUSION

This paper has presented the analysis of a static converter system able to process photovoltaic energy and feed it to the grid. The converter uses fewer switches when compared to similar ones presented in the literature, presents low harmonic distortion at the point of coupling connection, and galvanic isolation from the grid.

Other important features are: its robustness to short circuit, simple control strategy and low cost technology.

Due to its modularity many systems can be connected to the grid in a distributed generation.

IX. ACKNOWLEDGEMENT

Authors wish to thank Companhia Energética do Ceará - COELCE and Ceará State Research Foundation - FUNCAP for financially supporting that research.

X. REFERENCES

- [1] K. Harada, M. Sakamoto and M. Shoyama, (1987) "Phase controlled DC-AC converter with high frequency switching", IEEE PESC conf. Rec., pp 13-19.
- [2] Andersen, M., Alvsten, B. (1995). "200W Low Cost Module Integrated Utility Interface for Modular Photovoltaic Energy Systems", IEEE, pp 572-577.
- [3] Chiang, S. J., Chang, K. T., Yen, C. Y. " Residential Photovoltaics Energy Estorage System", IEEE Trans. On Industrial Electronics, vol. 45, N° 3, June 1998.
- [4] Calais, M., Agelides, V. G., "Multilevel Converters For Single-Phase Grid Connected Photovoltaic Systems – An Overview", IEEE ISIE'98, July 1998, pp. 224-229.
- [5] Denizar, M. C., Demonti, R., "Interconnection of a Photovoltaic Panel Array to a Single-Phase Utility Line from a Static Conversion System", IEEE ISIE'00, pp. 1207-1211.
- [6] Isoda, Hiroshi; Kimura, Ginji; Shioya, Mitsuo; Oshato, Massato H.; Battery Charging Characteristics in Small Scaled Photovoltaic Systems Using Resonant DC-DC Converter with Electrical Isolation; IECON90; California, USA, November, 1990; Vol. 2; p. 1118-1123.
- [7] Calais, R.; Al-haddad, K.; Rajagopalan, V.; A 5kW Utility-Interactive Inverter operating at High Frequency and using Zero Current Turn off COMFET Switches; Industry Application Society – IAS; Seattle, Washington, USA, October, 1999; p. 1-4.
- [8] Hussein, K. H.; Muta, I.; Hoshino, T.; Osakada, M.; IEE Proceeding; Genaration, Transmission and Distribution, volume 142, pags. 59 – 64; IEE, Stevenage, Herts.,U.K., january 1995.